



# Dynamic study of the gain in two beam coupling in photorefractive materials

T.K. Yadav\*, M.K. Maurya, R.A. Yadav

Laser and Spectroscopy Laboratory, Department of Physics, Banaras Hindu University, Varanasi 221005, India

## ARTICLE INFO

### Article history:

Received 19 January 2011

Accepted 16 June 2011

### Keywords:

Photorefractive materials

Index grating

Degenerate and non-degenerate two-beam coupling

## ABSTRACT

Wave equations describing the non-linear two-beam coupling have been solved and expressions for the gain of the two beams in the photorefractive crystals have been derived. In case of the degenerate two-beam coupling, the gain depends upon the crystal thickness, coupling coefficient, absorption coefficient and the input intensity ratio. The effect of these parameters on the gain has been studied in details. In case of non-degenerate two-beam coupling the gain not only depends upon crystal thickness, coupling coefficient, absorption coefficient and the input intensity ratio but also on the response time of the photorefractive medium. This response time is the function of concentration ratio. The influence of oscillation frequency shift, concentration ratio on the gain for the non-degenerate two-beam coupling has also been studied.

© 2012 Elsevier GmbH. All rights reserved.

## 1. Introduction

Two beams coupling in photorefractive crystal has been an active field of research in recent years because of its potential application such as signal processing, optical communications, optical networks, optical computing, real-time holography, image amplification, laser beam steering, optical interconnections, and holographic memory [1–6]. In two-beam coupling there are two beams of coherent electromagnetic radiation which intersect inside the photorefractive medium causing a periodic variation of the intensity due to interference which induces volume index grating. Presence of such an index grating affects the propagation of these two beams and is responsible for the beam coupling in photorefractive crystals. The most common theoretical description of the beam coupling in photorefractive materials is known as the coupled wave theory [7–11]. Photorefractive beam coupling is the non-linear interaction of phase and energy between the two beams in the photorefractive medium, where transfer of power from one beam to another takes place [12–16]. Through the photorefractive effect the interference pattern of the two beams is transformed into a refractive index grating [17,18]. The index grating can be considered as a dynamic volume grating, which is both formed by the beams and diffracts them, leading to non-linear beam coupling, which results in transfer of energy and phase between the two interacting beams. This energy transfer (beam coupling) between the beams in photorefractive crystals takes place due to a permanent phase mismatch between the refractive index grating and the incident light intensity grating. Maximum energy transfer is

obtained when the incident fringe pattern and the photo-induced index change are shifted by  $(\pi/2)$  (in the case of diffusion only) [19–22]. Direction of the energy transfer between the two beams is governed by the sign of the coupling constant. Two wave mixing gain is an important and useful parameter in photorefractive materials. But in case of the non-degenerate two-beam coupling, the gain depends on response time of the moving grating and it has been calculated regarding band transport model.

In the present paper we theoretically analyze the gain in case of non-linear co-directional and contra-directional two-beam coupling inside the photorefractive materials having absorbing properties under the slowly varying amplitude approximation [11]. In case of degenerate two-beam coupling the gain is the function of crystal thickness, coupling coefficient, absorption coefficient and the input intensity ratio. In the earlier published literature effects of these parameters on the gain have not been explored in details. But in case of non-degenerate two-beam coupling the gain not only depends upon crystal thickness, coupling coefficient, absorption coefficient and the input intensity ratio but also on the oscillation frequency shift and the response time of the photorefractive medium. This response time is the function of characteristic time constant of the medium, the diffusion field, the saturation field and drift field. The characteristic time constant of the medium depends on concentration ratio. Moreover, the effects of the oscillation frequency shift and concentration ratio of the materials on the gain have not been considered earlier. In this paper the above effects are considered in details.

## 2. Theoretical description

When two laser beams of same frequency progress in a photorefractive medium a stationary interference fringe pattern is formed,

\* Corresponding author.

E-mail address: [77.tarun@gmail.com](mailto:77.tarun@gmail.com) (T.K. Yadav).

however, when the frequencies of the two laser beams are different, the interference fringe pattern is no longer stationary. A volume index grating can still be induced provided the fringe pattern does not move too fast. The amplitude of the index modulation decreases as the speed of the fringe pattern increases. This is related to the finite time needed for the formation of index grating in the photorefractive medium. Let  $\omega_p$  and  $\omega_s$  be the frequency of the pump beam and signal beam respectively. The electric fields  $E_p$  and  $E_s$  of the two coupling beams can be written as,

$$E_p = A_p \exp[j(\omega_p t - \vec{k}_p \cdot \vec{r})] \tag{1}$$

$$E_s = A_s \exp[j(\omega_s t - \vec{k}_s \cdot \vec{r})] \tag{2}$$

where  $A_p$  and  $A_s$  are the amplitudes and  $\vec{k}_p$  and  $\vec{k}_s$  are the wave vectors of the pump and signal beams respectively,  $j = \sqrt{-1}$ , and  $t$  and  $r$  are the time and space coordinates respectively.

The intensity of the resultant electromagnetic radiation can be written as,

$$I = |A_p|^2 + |A_s|^2 + A_p^* A_s e^{j(\Omega t - \vec{k} \cdot \vec{r})} + A_p A_s^* e^{-j(\Omega t - \vec{k} \cdot \vec{r})} \tag{3}$$

$$I = I_0 + \text{Re}\{I_1 e^{j(\Omega t - \vec{k} \cdot \vec{r})}\}$$

where

$$I_0 = |A_p|^2 + |A_s|^2 = I_p + I_s$$

$$I_1 = 2A_s \cdot A_p^* = 2\sqrt{I_s I_p}$$

and the quantities  $\Omega$  and  $\vec{k}$  appearing in Eq. (3) are defined as,

$$\Omega = \omega_s - \omega_p \tag{4}$$

$$\vec{k} = \vec{k}_s - \vec{k}_p \tag{5}$$

The intensity distribution given by Eq. (3) represents a travelling fringe pattern moving with a speed

$$v = \frac{\Omega}{k} = \frac{\Omega \Lambda}{2\pi} \tag{6}$$

where  $\Lambda$  is the period of the fringe pattern. The index of refraction including the fundamental component of the intensity induced grating can be written [23] as,

$$n = n_0 + \left[ \frac{n_1}{2} \exp(j\Phi) \frac{A_p^* A_s}{I_0} \exp(j(\Omega t - \vec{k} \cdot \vec{r})) \right] + \text{c.c} \tag{7}$$

where  $\Phi$  is real and  $n_1$  is a real and positive number. A scalar grating is considered for the sake of convenience. The phase  $\Phi$  indicates the degree to which the index grating is shifted spatially with respect to the light interference pattern [24,25]. Thus, the values of  $\Phi$  and  $n_1$  can be written as,

$$\Phi = \Phi_0 + \tan^{-1}(\Omega \tau) \tag{8}$$

$$n_1 = \frac{2\Delta n_s}{\sqrt{(1 + \Omega^2 \tau^2)}} \tag{9}$$

where,  $\Delta n_s$  is the saturation value of the photo-induced index change. The parameters  $\Delta n_s$  and  $\Phi_0$  is a constant phase shift related to the non-local response of the crystal under the interference fringe illumination and depend not only on the grating spacing  $\Lambda$  and its direction but its material properties also e.g., the electro-optic coefficients and therefore, on the applied electric field. In photorefractive medium that operates by diffusion only (i.e., no external static electric field) the magnitude of  $\Phi_0$  is equal to  $(\pi/2)$  [26,27] (e.g., barium titanate (BaTiO<sub>3</sub>) crystal) with its sign depending upon the direction of the  $c$ -axis. The parameter  $\tau$  appearing in Eqs. (8) and (9) is the response time of the photorefractive medium [26]. On the basis of band transport model in which the materials

rate equations are solved for moving grating under the assumption  $I_1 \ll I_0$  the response time  $\tau$  is given by the relation [28,29].

$$\tau = t_0 = \frac{E_d + E_\mu}{E_d + E_q} \tag{10}$$

where  $t_0$  is a characteristic time constant of the medium,  $E_d$  is the diffusion field,  $E_q$  is the saturation field and  $E_\mu$  is another characteristic field (the so called drift field) and these are given by

$$t_0 = \frac{N_A}{N_D s I_0} \tag{11}$$

$$E_d = K \frac{K_B T}{q} \tag{12}$$

$$E_q = \frac{q N_A}{\epsilon_e K} \tag{13}$$

$$E_\mu = \frac{\gamma_r N_A}{\mu_e K} \tag{14}$$

where  $N_A$  is the density of acceptor impurities,  $N_D$  is the density of donor impurities,  $s$  is the cross-section of photo-excitation and  $K_B$  is the Boltzmann constant,  $T$  is the temperature,  $q$  is the electronic charge,  $\gamma_r$  is the recombination constant,  $\epsilon_e$  is the effective dielectric constant and  $\mu_e$  is the effective mobility. The expressions for  $\epsilon_e$  and  $\mu_e$  are given by the relation:

$$\epsilon_e = \frac{K \cdot \epsilon K}{K^2} \tag{15}$$

$$\mu_e = \frac{K \cdot \mu K}{K^2} \tag{16}$$

where,  $\epsilon$  is the dielectric constant of the photorefractive material and  $\mu$  is the mobility of the charge carriers [26]. The characteristic time constant  $t_0$  of the medium can also be written as,

$$t_0 = \frac{N_A}{N_D s I_0} = \frac{1}{r s I_0} \tag{17}$$

where  $r = N_D / N_A$  and is known as the concentration ratio. Using Eq. (17) the response time of the photorefractive medium  $\tau$  can be written as,

$$\tau = \frac{1}{r s I_0} \left( \frac{E_d + E_\mu}{E_d + E_q} \right) \tag{18}$$

In the case of two-beam coupling there are two beams of coherent electromagnetic radiation which intersect inside the photorefractive medium causing a periodic variation of the intensity due to interference which induces volume index grating. The response time  $\tau$  which is the function of diffusion field, the saturation field, characteristic field and concentration ratio play an important role in the formation of volume index grating. A finite spatial phase shift between the interference pattern and the induced volume index grating has been known for some time [19,20]. The presence of such a phase shift allows the possibility of the non-reciprocal steady-state transfer of energy between the two light beams. Steady state coupled wave equations for the degenerate two-beam coupling are given by [30].

$$\frac{dI_p}{dz} = - \left[ \frac{\gamma_0}{1 + \Omega^2 \tau^2} \right] \frac{I_p I_s}{I_p + I_s} - \alpha I_p \tag{19}$$

$$\frac{dI_s}{dz} = - \left[ \frac{\gamma_0}{1 + \Omega^2 \tau^2} \right] \frac{I_p I_s}{I_p + I_s} - \alpha I_s \tag{20}$$

$$\frac{d\Psi_p}{dz} = - \left[ \frac{\Omega \tau \gamma_0}{2(1 + \Omega^2 \tau^2)} \right] \frac{I_s}{I_p + I_s} \tag{21}$$

$$\frac{d\Psi_s}{dz} = - \left[ \frac{\Omega \tau \gamma_0}{2(1 + \Omega^2 \tau^2)} \right] \frac{I_p}{I_p + I_s} \tag{22}$$

where,  $\gamma_0$  is the coupling constant for the case of degenerate two wave mixing (i.e.,  $\Omega = \omega_p - \omega_s = 0$ ) and  $\alpha$  is the absorption coefficient of the materials. Adding Eqs. (19) and (20) and integrating with respect to  $z$  yields,

$$I_p(z) + I_s(z) = \{I_p(0) + I_s(0)\} \exp(-\alpha z) \tag{23}$$

Using Eq. (23), Eqs. (19) and (20) give the following differential equations:

$$\frac{dI_p}{dz} + \frac{\gamma_0}{I_0(1 + \Omega^2 \tau^2)} I_p^2 \exp(\alpha z) + \left( \frac{\gamma_0}{1 + \Omega^2 \tau^2} + \alpha \right) I_p = 0 \tag{24}$$

$$\frac{dI_s}{dz} + \frac{\gamma_0}{I_0(1 + \Omega^2 \tau^2)} I_s^2 \exp(\alpha z) - \left( \frac{\gamma_0}{1 + \Omega^2 \tau^2} + \alpha \right) I_p = 0 \tag{25}$$

where  $I_0 = I_p(0) + I_s(0)$ . Eqs. (24) and (25) can be integrated to yield the following equations:

$$I_p(z) = \frac{(1 + m) \exp(-\alpha z)}{m + \exp(\gamma_0/(1 + \Omega^2 \tau^2))} I_p(0) \tag{26}$$

$$I_s(z) = \frac{(1 + m) \exp(-\alpha z)}{1 + m \exp(-\gamma_0/(1 + \Omega^2 \tau^2))} I_s(0) \tag{27}$$

where,  $m$  is the input intensity ratio given by,

$$m = \frac{I_p(0)}{I_s(0)} \tag{28}$$

From Eq. (27) it is obvious that in the absence of the material absorption ( $\alpha = 0$ ), the intensity of the signal beam  $I_s(z)$  is an increasing function of  $z$ , whereas Eq. (26) shows that the intensity of the pump beam  $I_p(z)$  is a decreasing function of  $z$ . The energy

mixing, where the sum of the beam intensities is a constant of integration for the non-absorbing medium, in the contra-directional two-waves mixing, the difference of the beam intensities is a constant of integration. In addition, the forms of the coupled equations which govern the wave amplitudes also differ from those of the co-directional coupling case, leading to qualitative differences in the energy exchanges between the two waves in the two cases. The above two Eqs. (19) and (20) can be solved for the non-absorbing medium ( $\alpha = 0$ ) for which the difference of the two beam intensities  $I_s(0) - I_p(0)$  is a constant and for such a case these equations have the solutions [1],

$$I_p^{\alpha=0}(z) = f(z) - Q \tag{33}$$

$$I_s^{\alpha=0}(z) = f(z) + Q \tag{34}$$

where,  $Q$  and  $f(z)$  are given by,

$$Q = \frac{I_s(0) - I_p(0)}{2} \tag{35}$$

$$f(z) = \sqrt{Q^2 + P \exp\left(-\frac{\gamma_0 L}{1 + \Omega^2 [(1/rsI_0)((E_d + E_\mu)/(E_d + E_q))]\right)} \tag{36}$$

with the value of  $P$  given by,

$$P = I_p(0) I_s(0) \tag{37}$$

The constants  $P$  and  $Q$  can be more conveniently expressed in terms of initial intensities of the pump beam and signal beam, i.e.,  $I_p(0)$  and  $I_s(L)$  as,

$$P = I_p(0) I_s(L) \left\{ \frac{I_p(0) + I_s(L)}{I_s(L) + I_p(0) \exp((\gamma_0 L)/(1 + \Omega^2 [(1/rsI_0)((E_d + E_\mu)/(E_d + E_q))])^2)} \right\} \tag{38}$$

$$Q = \frac{1}{2} \left\{ \frac{I_s^2(L) - I_p^2(0) \exp((\gamma_0 L)/(1 + \Omega^2 [(1/rsI_0)((E_d + E_\mu)/(E_d + E_q))])^2)}{I_s^2(L) + I_p^2(0) \exp((\gamma_0 L)/(1 + \Omega^2 [(1/rsI_0)((E_d + E_\mu)/(E_d + E_q))])^2)} \right\} \tag{39}$$

transfer from the pump beam to the signal beam can be described by coupling constant  $\gamma_0$  whose sign depends on the direction of the  $c$ -axis. As a result of the coupling  $\gamma_0 > 0$  the signal beam gains energy from pump beam. In the presence of material absorption (i.e.  $\alpha > 0$ ), the signal beam can still be amplified provided the gain due to the beam coupling is large enough to overcome the losses.

The parametric two-wave mixing gain can be defined as,

$$g = \frac{I_s(L)}{I_s(0)} \tag{29}$$

Eqs. (27) and (29) lead to the following expression for  $g$ :

$$g = \frac{(1 + m) \exp(-\alpha L)}{1 + m \exp(-\gamma_0/(1 + \Omega^2 \tau^2))} \tag{30}$$

Substituting the value of  $\tau$  from Eq. (18) into Eq. (30) we have

$$g = \frac{(1 + m) \exp(-\alpha L)}{1 + m \exp(\gamma_0 L / (1 + \Omega^2 [(1/rsI_0)(E_d + E_\mu/E_d + E_q)]^2))} \tag{31}$$

For large  $m$ , i.e. in the beginning of the coupling, the terms  $(1 + m)$  and  $1 + m \exp(-\alpha L)$  in Eq. (31) can be approximated by  $m$  and  $m \exp(-\alpha L)$  respectively and therefore, the gain  $g$  can be written as,

$$g \approx \exp \left\{ \left( \frac{\gamma_0}{1 + \Omega^2 [(1/rsI_0)(E_d + E_\mu/E_d + E_q)]^2} - \alpha \right) L \right\} \tag{32}$$

From Eq. (32) we see that the amplification ( $g > 1$ ) is possible only when  $\gamma_0 / (1 + \Omega^2 [(1/rsI_0)(E_d + E_\mu/E_d + E_q)]^2) > \alpha$ .

When both the beams enter into the medium from the opposite sides the coupling is known as contra-directional two-wave coupling. Contrary to the case of the co-directional two-wave

According to Eqs. (26) and (27), both  $I_p(z)$  and  $I_s(z)$  are decreasing functions of  $z$ , provided  $\gamma$  is positive and  $\alpha = 0$ . Transmittances for both the waves are defined as,

$$t_p = \frac{I_p(L)}{I_p(0)} = \frac{(1 + m)}{m + \exp((\gamma_0 L)/(1 + \Omega^2 [(1/rsI_0)((E_d + E_\mu)/(E_d + E_q))])^2)} \tag{40}$$

$$t_s = \frac{I_s(0)}{I_s(L)} = \frac{(1 + m)}{1 + m + \exp(-(\gamma_0 L)/(1 + \Omega^2 [(1/rsI_0)((E_d + E_\mu)/(E_d + E_q))])^2)} \tag{41}$$

where  $m$  is the incident intensity ratio  $m = I_p(0)/I_s(L)$ . Note that  $t_p < 1$  and  $t_s > 1$  for positive  $\gamma$ . It is interesting to note that these expressions for the transmittances are formally identical to those of the co-directional coupling case even though the spatial variations of  $I_p(z)$  and  $I_s(z)$  with respect to  $z$  are very different. Note that  $t_p$  and  $t_s$  are related by  $t_s = t_p \exp(\gamma_0 L / (1 + \Omega^2 [(1/rsI_0)((E_d + E_\mu)/(E_d + E_q))])^2)$ .

### 3. Results and discussion

Eq. (31) is the analytical expression for the two-wave mixing gain for the whole ranges of modulation ratio  $m$  and it is clear

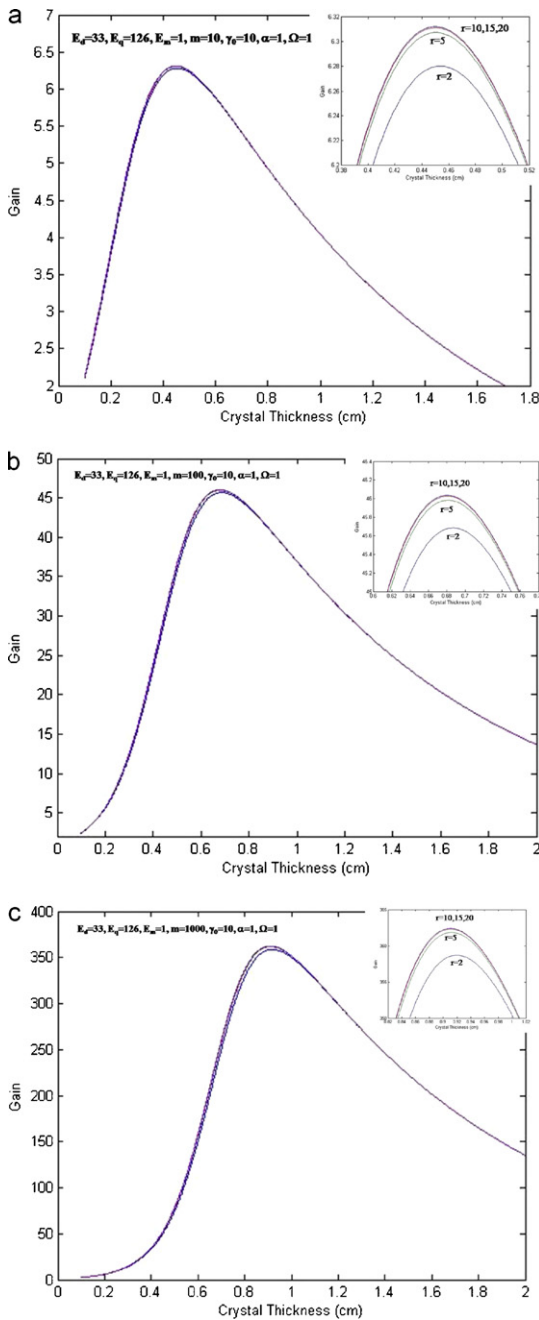


**Fig. 1.** Variation of gain with the crystal thickness for a constant value of  $E_d$  ( $=33$  kV/cm),  $E_q$  ( $=126$  kV/cm),  $E_m$  ( $=1$  kV/cm),  $\gamma_0$  ( $=10$  cm $^{-1}$ ),  $\alpha$  ( $=1$  cm $^{-1}$ ),  $\Omega$  ( $=1$  Hz) in the presence of absorption for different values of concentration ratio  $r$  ( $=N_D/N_A$ ) at various values of (a)  $m = 10$ , (b)  $m = 100$ , and (c)  $m = 1000$ .

that the two-beam coupling gain is not only a function of energy coupling coefficient, crystal thickness, modulation ratio, absorption coefficient and oscillation frequency shift but also a function of concentration ratio  $r$ . Variations of gain with the crystal thickness for constant values of  $E_d$  ( $=33$  kV/cm),  $E_q$  ( $=126$  kV/cm),  $E_m$  ( $=1$  kV/cm),  $\gamma_0$  ( $=10$  cm $^{-1}$ ),  $\alpha$  ( $=1$ ) and  $\Omega$  ( $=1$  Hz) for different values of concentration ratio  $r$  and  $m$  ( $=10, 100$  and  $1000$ ) are shown in Fig. 1a, b and c respectively. It is evident that the gain increases with increasing crystal thickness reaches a maximum and then decreases exponentially due to the material absorption. For lower value of concentration ratio, the gain depends upon the concentration ratio ( $r < 10$ ) but for higher values of  $r$  ( $\geq 10$ ) the gain is

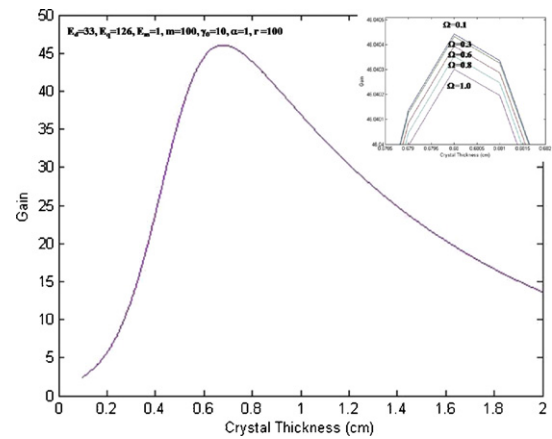


**Fig. 2.** Variation of gain with crystal thickness for a constant value of  $E_d$  ( $=33$  kV/cm),  $E_q$  ( $=126$  kV/cm),  $E_m$  ( $=1$  kV/cm),  $m$  ( $=10$ ),  $\gamma_0$  ( $=10.0$  cm $^{-1}$ ),  $\alpha$  ( $=1$  cm $^{-1}$ ),  $r = 100$ , for different values of  $\Omega$  ( $=0.1, 0.3, 0.6, 0.8, 1.0$ ).

independent of concentration ratio  $r$ . Moreover for larger value of  $m$  the gain is larger Fig. 1(a–c).

Variation of gain with crystal thickness for constant values of  $E_d$  ( $=33$  kV/cm),  $E_q$  ( $=126$  kV/cm),  $E_m$  ( $=1$  kV/cm),  $m$  ( $=10$ ),  $\gamma_0$  ( $=10.0$  cm $^{-1}$ ),  $\alpha$  ( $=1$  cm $^{-1}$ ),  $r = 100$ , for different values of  $\Omega$  ( $=0.1, 0.3, 0.6, 0.8, 1.0$  Hz) is shown in Fig. 2. The gain increases with the crystal thickness and the optimum gain occurs at an appropriate interaction length, beyond which the gain starts decreasing exponentially due to materials absorption. It is found that the gain is almost independent of the oscillation frequency shift. Thus, the optimum gain occurs at the same interaction length ( $L = 0.68$  cm) for the different values of  $\Omega$  ( $=0.1, 0.3, 0.6, 0.8, 1.0$  Hz).

Fig. 3 shows variation of gain with the crystal thickness for constant values of  $E_d$  ( $=33$  kV/cm),  $E_q$  ( $=126$  kV/cm),  $E_m$  ( $=1$  kV/cm),  $r$  ( $=100$ ),  $\gamma_0$  ( $=20$  cm $^{-1}$ ),  $\alpha$  ( $=1$  cm $^{-1}$ ),  $\Omega$  ( $=1$  Hz) at different values of modulation ratio ( $r$ ). With the increasing value of the crystal thickness the gain increases rapidly, at certain crystal thickness it becomes optimum and then decreases due to material absorption. The optimum gain value is found to be larger for the larger value of modulation ratio. For the lower value of  $m$  the optimum value of the gain is observed at the lower values of crystal thickness.

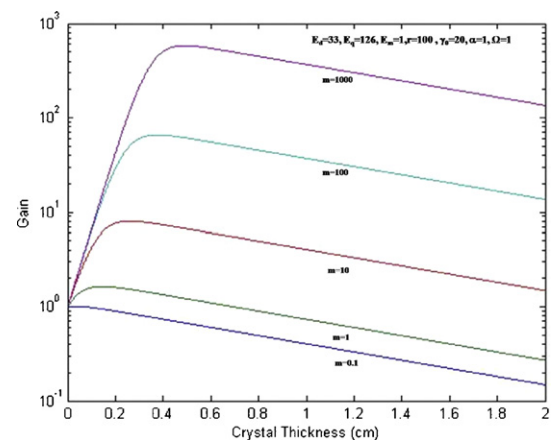


**Fig. 3.** Variation of gain with the crystal thickness for a constant value of  $E_d$  ( $=33$  kV/cm),  $E_q$  ( $=126$  kV/cm),  $E_m$  ( $=1$  kV/cm),  $r$  ( $=100$ ),  $\gamma_0$  ( $=20$  cm $^{-1}$ ),  $\alpha$  ( $=1$  cm $^{-1}$ ),  $\Omega$  ( $=1$  Hz) at different values of modulation ratio.

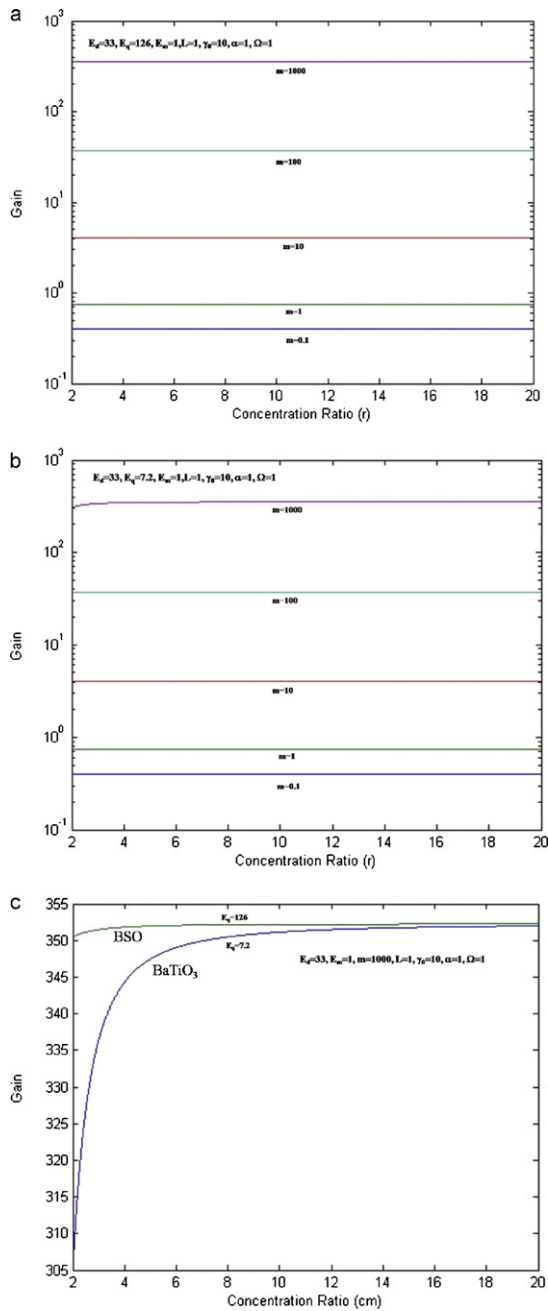


**Fig. 4.** Variation of gain with concentration ratio ( $r$ ) for a constant value of  $E_d$  ( $=33$  kV/cm),  $E_q$  ( $=126$  kV/cm),  $E_m$  ( $=1$  kV/cm),  $\gamma_0$  ( $=10.0$  cm<sup>-1</sup>),  $\alpha$  ( $=1$  cm<sup>-1</sup>),  $L$  = 1 cm, for different values of  $m$  ( $=0.1, 1, 10, 100$  and  $1000$ ) for (a) BSO material; (b) BaTiO<sub>3</sub> material; and (c) comparison of gain for BSO and BaTiO<sub>3</sub> materials.

Fig. 4a and b shows the variation of gain with concentration ratio ( $r$ ) for constant values of  $E_d$  ( $=33$  kV/cm),  $E_q$  ( $=126$  kV/cm),  $E_m$  ( $=1$  kV/cm),  $\gamma_0$  ( $=10.0$  cm<sup>-1</sup>),  $\alpha$  ( $=1$  cm<sup>-1</sup>),  $L$  = 1 cm, for different values of  $m$  ( $=0.1, 1, 10, 100$  and  $1000$ ) for different materials BSO (Bi<sub>12</sub>SiO<sub>20</sub>) and BaTiO<sub>3</sub> respectively. For the lower values of modulation ratios ( $m$ ) the gain is unaltered with concentration ratio but for higher values of  $m=1000$  the gain is affected by concentration ratio and it increases with increasing concentration ratio and reaches its saturation value. In order to compare the variations of gain with  $r$  for BSO and BaTiO<sub>3</sub> materials we have plotted in Fig. 4c against  $r$  for  $m=1000$ . One can see that the gain increases with increasing concentration ratio and gain is higher for BSO at lower values of concentration ratio than the

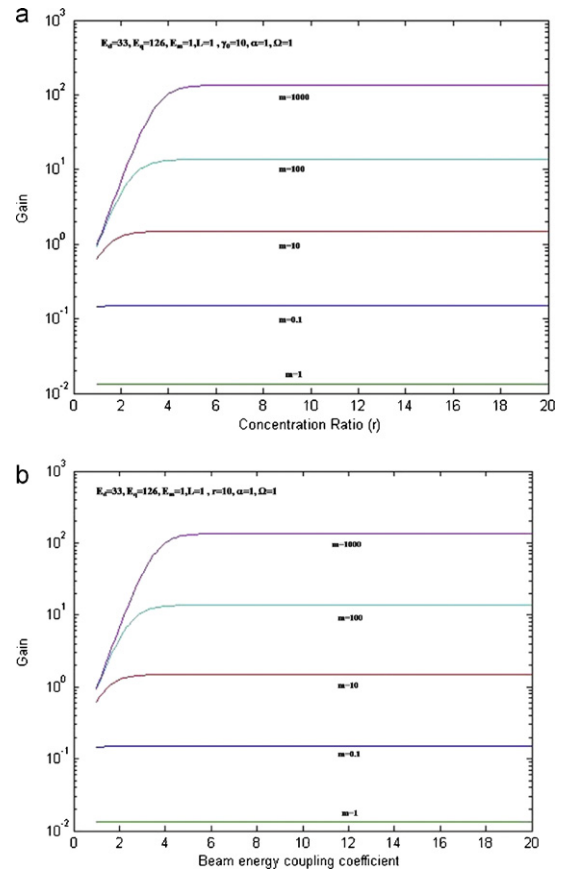


**Fig. 5.** Variation of gain with the crystal thickness for a constant value of  $E_d$  ( $=33$  kV/cm),  $E_q$  ( $=126$  kV/cm),  $E_m$  ( $=1$  kV/cm),  $m$  ( $=10$ ),  $\gamma_0$  ( $=10$  cm<sup>-1</sup>),  $\alpha$  ( $=1$  cm<sup>-1</sup>),  $\Omega$  ( $=1$  Hz) for different values of  $\alpha$ .

BaTiO<sub>3</sub> material it due to the higher value of dielectric constant of BSO.

Variation of gain with the concentration ratio and beam energy coupling for a constant value of  $E_d$  ( $=33$  kV/cm),  $E_q$  ( $=126$  kV/cm),  $E_m$  ( $=1$  kV/cm),  $\alpha$  ( $=1$  cm<sup>-1</sup>),  $\Omega$  ( $=1$  Hz) are shown in Fig. 5a and b respectively. The gain increases with the increasing value of concentration ratio reaches its saturation value. For larger value of input intensity ratio the gain is larger. Similar variation of gain is observed with beam energy coupling coefficient and is higher for higher values of  $m$ .

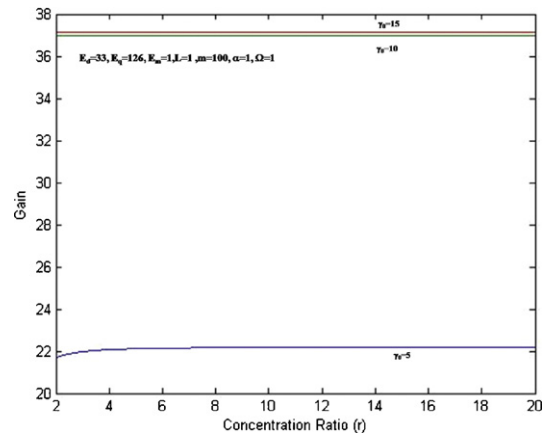


**Fig. 6.** Variation of gain with the concentration ratios for a constant value of  $E_d$  ( $=33$  kV/cm),  $E_q$  ( $=126$  kV/cm),  $E_m$  ( $=1$  kV/cm),  $m$  ( $=100$ ),  $L$  ( $=1$  cm),  $\alpha$  ( $=1$  cm<sup>-1</sup>),  $\Omega$  ( $=1$  Hz) at different values of coupling coefficient  $\gamma_0$  ( $=5, 10, 15$  cm<sup>-1</sup>).

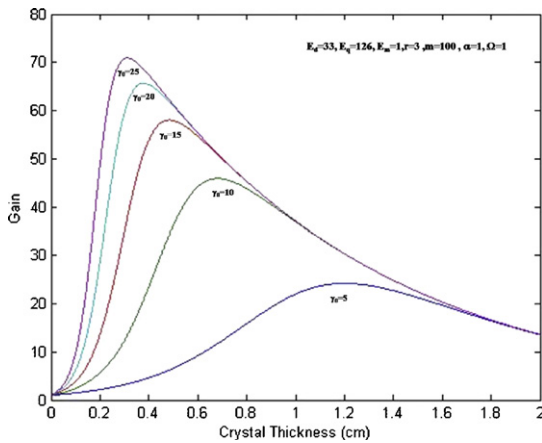


**Fig. 7.** Variation of gain with the crystal thickness of the materials for different values of energy coupling coefficient with the fixed values of  $E_d$  ( $=33$  kV/cm),  $E_q$  ( $=126$  kV/cm),  $E_m$  ( $=1$  kV/cm),  $\gamma_0$  ( $=10.0$  cm $^{-1}$ ),  $m$  ( $=100$ ),  $\alpha$  ( $=1$  cm $^{-1}$ ),  $\Omega$  ( $=1$  Hz).

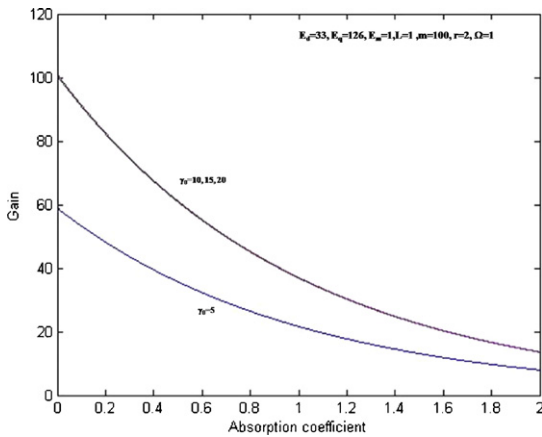


**Fig. 8.** Variation of gain with the absorption coefficient for a constant value of  $E_d$  ( $=33$  kV/cm),  $E_q$  ( $=126$  kV/cm),  $E_m$  ( $=1$  kV/cm),  $m$  ( $=100$ ),  $r$  ( $=100$ ), and  $\Omega$  ( $=1$  Hz) for different values of coupling coefficient  $\gamma_0$  ( $=5, 10, 15, 20$  cm $^{-1}$ ).

Variations of gain with the concentration ratios for constant values of  $E_d$  ( $=33$  kV/cm),  $E_q$  ( $=126$  kV/cm),  $E_m$  ( $=1$  kV/cm),  $m$  ( $=100$ ),  $L$  ( $=1$  cm),  $\alpha$  ( $=1$  cm $^{-1}$ ),  $\Omega$  ( $=1$  Hz) at different values of coupling coefficient  $\gamma_0$  ( $=5, 10, 15$  cm $^{-1}$ ) are shown in Fig. 6. For lower value of  $\gamma_0$  ( $=5$  cm $^{-1}$ ) the gain increases with increasing concentration ratio and afterwards it saturates. It is interesting to note that for higher values of  $\gamma_0$  ( $=10, 15$  cm $^{-1}$ ) the gain is independent of concentration ratio. Thus for the larger values of coupling coefficient, the concentration ratio ( $r = N_D/N_A$ ) is ineffective.

Fig. 7 is a plot of the two-wave mixing gain as a function of crystal thickness of the material for different values of energy coupling coefficient with fixed values of  $E_d$  ( $=33$  kV/cm),  $E_q$  ( $=126$  kV/cm),  $E_m$  ( $=1$  kV/cm),  $\gamma_0$  ( $=10.0$  cm $^{-1}$ ),  $m$  ( $=100$ ),  $\alpha$  ( $=1$  cm $^{-1}$ ),  $\Omega$  ( $=1$  Hz). From Fig. 7 it is obvious that the gain increases as the crystal thickness increases and reaches a maximum value and then decreases exponentially due to material absorption. The gain is higher for the higher values of energy coupling coefficient. Also, the gain peak height increases with increasing value of coupling coefficient and it is shifted towards the lower values of crystal thickness.

The dependence of the co-directional two-beam coupling gain  $g$  on the absorption coefficient  $\alpha$  is shown in Fig. 8 which shows the variation of gain with the absorption coefficient for constant values of  $E_d$  ( $=33$  kV/cm),  $E_q$  ( $=126$  kV/cm),  $E_m$  ( $=1$  kV/cm),  $m$  ( $=100$ ),  $r$  ( $=100$ ), and  $\Omega$  ( $=1$  Hz) for different values of coupling coefficient

$\gamma_0$  ( $=5, 10, 15, 20$  cm $^{-1}$ ). It is clear that with the increasing value of the absorption coefficient the gain decreases rapidly and it is higher for the higher values of coupling coefficient. However, for longer for  $\gamma_0$  ( $=10, 15$  and  $20$  cm $^{-1}$ ) there is no variation of  $g$  with  $\gamma_0$ .

#### 4. Conclusions

The two wave mixing gain is an important and useful parameter in photorefractive materials and it is not only the function of energy coupling coefficient, crystal thickness, modulation ratio, absorption coefficient and oscillation frequency shift but also the function of concentration ratio ( $r = N_D/N_A$ ) and oscillation frequency shift. For lower values of concentration ratio the gain depends upon the concentration ratio ( $r < 10$ ) but for higher values ( $r \geq 10$ ) the gain is independent of concentration ratio. The gain increases with increasing concentration ratio and it is observed that the gain is higher for BSO at lower values of concentration ratio than that of the BaTiO<sub>3</sub> material. Thus the response of the BSO is better than that of BaTiO<sub>3</sub> at very high modulation ratio  $m = 1000$ . For lower value of coupling coefficient the gain increases with increasing concentration ratio and the gain is almost independent of oscillation frequency shift. For higher values the gain is independent of concentration ratio. For the larger values of coupling coefficient, the concentration ratio is ineffective as far as the gain is concerned.

#### Acknowledgment

Two of the authors (TKY and MKM) acknowledge financial support from CSIR New Delhi during the research period in the form of senior research fellowships.

#### References

- [1] P. Yeh, Introduction to Photorefractive Nonlinear Optics, Wiley, New York, 1993, 118–141.
- [2] P. Gunter, J.P. Huignard, Photorefractive Materials and their Applications, Vols. I–II, Springer, New York, 1988.
- [3] M. Cronin-golomb, B. Fischer, J.O. White, A. Yariv, J. Opt. Soc. Am. B 71 (1981) 1564.
- [4] K. Paivasaari, A.A. Kamshilin, P. Delaye, G. Roosen, Opt. Commun. 213 (2002) 357–366.
- [5] Z.Y. Li, B.Y. Gu, G.Z. Yang, J. Phys. Rev. B 60 (1999) 10644–10647.
- [6] I.C. Khoo, Liquid crystal photorefractive optics: dynamic and storage holographic grating formation wave, mixing, and beam/image processing, Photorefract. Opt. (2000) 75–104.
- [7] J.M. Jarem, P.P. Banerjee, Opt. Commun. 123 (1996) 825–842.
- [8] M. Chauvet, T. Towe, G.J. Salamo, D.F. Bliss, G. Bryant, G. Iseler, Opt. Commun. 134 (1997) 211–217.
- [9] L.M. Connors, T.J. Hall, M.A. Fiddy, Appl. Phys. B 28 (1982) 31; H.K. Bell, J. Tech. Syst. 48 (1969) 2909; Y. Jiang, Y. Li, Z. Xiudong, S. Zhou, K. Xu, Appl. Phys. 82 (1997) 2017–2022.
- [10] K.R. MacDonald, J. Feinberg, Z.Z. Ming, P. Günter, Opt. Commun. 50 (1984) 146.
- [11] N.V. Kukhtarev, V.B. Markov, S.G. Odulov, M.S. Soskin, V.L. Vinetskii, Ferroelectrics 22 (1979) 949.
- [12] M.C. Søren, B. Jensen, J.P. Huignard, P.M. Petersen, Opt. Express 14 (2006) 12373–12379.
- [13] M.C. Søren, B. Jensen, J.P. Huignard, P.M. Petersen, Opt. Express 16 (2008) 5565–5571.
- [14] A.V. Khomenko, I. Rocha-Mendoza, Phys. Rev. E 70 (2004) 066615.
- [15] I. de Oliveira, J. Frejlich, Phys. Rev. A 64 (2001) 033806.
- [16] P. Vaveliuk, B. Ruiz, N. Bolognini, J. Fernandez, Phys. Rev. B 62 (2000) 4511.
- [17] V.L. Vinetskii, N.V. Kukhtarev, S.G. Odulov, M.S. Soskin, Sov. Phys. Usp 22 (1979) 742–756.
- [18] C. Xin, L. Jin-Song, W. Sheng-Lie, L. Shi-Xiong, Chin. Phys. B 18 (2009) 1891–1897.
- [19] D.L.J. Staebler, J. Amodi Appl. Phys 43 (1972) 1042–1049.
- [20] N. Khelfaoui, D. Wolfersberger, G. Kugel, N. Fressengeas, M. Chauvet, Opt. Commun. 261 (2006) 169–174.
- [21] R.K. Banyal, B.R. Prasad, J. Indian Inst. Sci. 83 (2003) 61–71.
- [22] J.S. Liu, Opt. Lett. 28 (2003) 2237.

- [23] B. Fischer, M. Cronin-Golomb, J.O. White, A. Yariv, *Opt. Lett.* 6 (1981) 519–521.
- [24] J.P. Huignard, A. Marrackchi, *Opt. Commun.* 38 (1981) 249.
- [25] L. Mosquera, I. de Oliveira, J. Frejich, A.C. Hernandez, S. Lanfredi, J.F. Carvalho, *J. Appl. Phys.* 90 (2001) 2635–2641.
- [26] P. Yeh, *Introduction to Photorefractive Nonlinear Optics*, Wiley, New York, 1993.
- [27] N.V. Kukhtarev, V.B. Markov, S.G. Odulov, M.S. Soskin, V.L. Vinetskii, *Ferroelectrics* 22 (1979) 961.
- [28] C.H. Kwak, S.Y. Park, J.S. Jeong, H.H. Suh, E.H. Lee, *Opt. Commun.* 105 (1994) 353–358.
- [29] C.H. Kwak, S.Y. Park, E.H. Lee, *Opt. Commun.* 115 (1995) 315–322.
- [30] M.K. Maurya, T.K. Yadav, R.A. Yadav, *Opt. Laser Technol.* 42 (2010) 465–476.